Mesoscopic Simulation of the Surface Inducing Effects on the Compatibility of PS-*b*-PMMA Copolymers

Dan Mu,[1] Jian-Quan Li,[2] Song Wang[3]

[1]*College of Chemistry Chemical Engineering and Materials Science, Zaozhuang University, Shandong 277160, China*
[2]*Photoelectric Engineering College, Zaozhuang University, Shandong 277160, China*
[3]*Institute of Theoretical Chemistry, State Key Laboratory of Theoretical and Computational Chemistry, Jilin University, Changchun 130023, China*

Received 29 March 2011; accepted 20 June 2011
DOI 10.1002/app.35121
Published online 10 October 2011 in Wiley Online Library (wileyonlinelibrary.com).

ABSTRACT: The phase morphologies of designed polystyrene-*block*-poly(methyl methacrylate) (PS-*b*-PMMA) copolymers were studied at 383, 413, and 443 K by mesoscopic simulations. Eighteen patterned surfaces of four series were designed and designated as "ci," "co," "gra," and "rg" to study their influence on changing the microscopic phase morphology of copolymers. The topography of the "ci" series surfaces was shaped by semicircular balls. Different radii were applied to simulate different degrees of surface roughness. The "co" series were composed of cubic columns as the mask, and the cubic columns were separated by equal spaces. Various sizes and heights of columns were used to simulate different degrees of surface roughness. The "gra" series were composed of surfaces with different areas of section and the same height to simulate different degrees of surface roughness. The "rg" series were composed of concentric cuboids with continuous increasing heights and sizes. The degree of phase separation depended on the structures of copolymers, the topography of surfaces and the simulation temperatures. When the triblock copolymer with surfaces induced was composed of the same component at both ends and had larger PS segment percentage, it would present higher values of order parameter, that was, "ABA" showed the highest, "AB" the second high and "BAB" the last, the values of order parameter of the long chains were higher than those of the short ones, except the situation with co-4432 and co-8832 surfaces induced. However, the co-4432 and co-8832 surfaces performed the most intensive extent of inducing effect. J Appl Polym Sci 124: 879–889, 2012

Key words: block copolymers; calculations; computer modeling

INTRODUCTION

Block copolymers are macromolecules composed of sequences of chemically distinct and mutually incompatible sequence of reapeat units that are covalently bonded. They tend to form various ordered morphologies which are in general on the nanometer scale through self-assembly and microphase separation. Recently, a number of works have focused on the phase behavior of block copolymer and their intriguing properties in research areas, such as supramolecular chemistry, materials science, and nanotechnology.[1–13] Self-assembly of block copolymers depends on molecular weight, segment size, and the strength of interaction between the blocks, represented by the Flory-Huggins interaction parameter, χ. The morphology depends on χ, the composition of the copolymers and the volume fraction of one of the constituent blocks.[14,15] Thus block copolymers have attracted many researchers' attention in both theoretical and application fields.[16–21]

PS/PMMA binary blends are a well-known immiscible combination,[22–29] and can be observed bulk and surface phase separation.[30,31] Polystyrene-*block*-poly(methyl methacrylate) (PS-*b*-PMMA) copolymer is a polymer composed of two immiscible polymers blocks, which was studied in our former work; we had obtained the representative chain lengths of PS and PMMA chain, the χ data of 10 different compositions which can cover most compositions at 383, 413, and 443 K[32], and these data could be applied as the input parameters to deal with the PS-*b*-PMMA copolymers in this work. The connection between the microscale and the mesoscale was as follows:

$$IPM = \chi_{ab} RT,$$

where the parameter χ_{ab} was calculated by atomistic simulation for each blend composition at different temperature. R is the molar gas constant,

Correspondence to: D. Mu (mudanjlu1980@yahoo.com.cn).
Contract grant sponsor: Promotive Research Fund for Excellent Young and Middle-aged Scientists of Shandong Province; contract grant number: BS2010CL048.
Contract grant sponsor: Shandong Province Higher School Science and Technology Fund Planning Project; contract grant number: J10LA61.
Contract grant sponsor: Zaozhuang Scientific and Technological Project; contract grant number: 200924-2.

TABLE I
Details of the Designed PS-*b*-PMMA Copolymers Models

Classified group	System	wt% of PMMA content	IPM[a] (383K)	IPM[a] (413K)	IPM[a] (443K)
"AB" group	A3B6	66.01	0.92057	0.91268	1.02383
	A6B12	66.01	0.92057	0.91268	1.02383
"ABA" group	A3B6A3	49.04	0.59536	0.74319	0.80883
	A6B12A6	49.04	0.59536	0.74319	0.80883
"BAB" group	B6A3B6	79.13	1.07334	1.15849	1.13485
	B12A6B12	79.13	1.07334	1.15849	1.13485

[a] IPM was the abbreviation for "Input Parameter of MesoDyn".

8.314 J · mol^{-1}· K^{-1}, and T was the simulation temperature. IPM was the abbreviation of "Input Parameter of MesoDyn" used to describe the interaction between beads.[32]

Mesoscopic dynamics models have been receiving increasing attention, as they form a bridge between micro-scale and macro-scale properties.[33–36] Compared with atomistic simulation methods, the mesoscopic dynamics (MesoDyn)[37–39] can largen the scale of the simulation by several orders of magnitude, which can deal with the polymer chain at a mesoscopic level by grouping atoms together and then coarse-graining them to be persistent length polymer chains. It utilizes dynamic mean-field density functional theory (DFT), in which the dynamics of phase separation can be described by Langevin-type equations to investigate polymer diffusion. The most important molecular parameter is the "incompatibility parameter" χN, where χ is the Flory-Huggins interaction parameter and N is the degree of polymerization. Therefore, the MesoDyn method can be considered as a reliable method to deal with PS-*b*-PMMA copolymers. The mesoscale simulations in this paper were all carried out with the MesoDyn module in the Material Studio commercial software provided by Accelrys.

The mesoscopic simulations in this article were all related to the surface inducing effects on the compatibility of PS-*b*-PMMA copolymers. It mainly contained the calculations of the surface inducing effects on changing the phase morphology of the PS-*b*-PMMA copolymers at 383, 413, and 443 K. Thus, our study results would be a strong proof from theoretical view.

MODELS AND SIMULATIONS

Models

To study the compatibility of different PS-*b*-PMMA copolymers, six types of copolymers denoted as A3B6, A6B12, A3B6A3, A6B12A6, B6A3B6, and B12A6B12 were designed, in which A and B represented PS and PMMA segments, respectively. For convenience, A3B6 and A6B12 were defined as the "AB" groups; A3B6A3 and A6B12A6 were defined as the "ABA" group; B6A3B6 and B12A6B12 were defined as the "BAB" group. The former of each group represented short PS-*b*-PMMA copolymer chains and the latter represented long ones; the chain length of the latter was twice as long as the former in the same group. Six types of copolymer models were given in Table I in detail. The classified group information, the weight percentages of PMMA content and the input parameters of MesoDyn at 383, 413, and 443 K[32] were also listed in this table.

We designed four series patterned surfaces as substrates, designated as "ci," "co," "gra," and "rg" series, to study its inducing effects on the compatibility of PS-*b*-PMMA copolymers. The "ci" series of planes used half-spheres with different radii as a mask that simulated different degrees of surface roughness. The "co" series had equally spaced cubic columns as a mask. The

TABLE II
Information of "ci," "co," "gra," and "rg" Series Surfaces

Type	Included Surfaces	Example	Scheme	Mask Type	Name Explanation
ci-xxx	ci-444, ci-882	ci-444	S1	Semicircular balls	Four semicircular balls in four surface sides, the radius is 4 nm
co-4xx	co-444, co-448, co-4412, co-4432	co-444	S2	Equal spaced cubic columns	Divided by equal space into four parts to form two columns in four surface sides, the height is 4 nm
co-8xx	co-884, co-888, co-8812, co-8832	co-884	S3	Equal spaced cubic columns	Divided by equal space into eight parts to form four columns in four surface sides, the height is 4 nm
gra-xxx	gra-444, gra-888	gra-444	S4	The same widths, gradually increasing height columns, monodirectional asymmetric	Divided by equal space into four parts in face-to-face sides to four small surfaces with gradually increasing height, the highest height is 4 nm
gra-2(xxx)	gra-2(444), gra-2(448), gra-2(888)	gra-2(444)	S5	The same as gra-xxx type, but monodirectional symmetric	With the same two symmetric parts as gra-444 surface
rg-xxx	rg-442, rg-884, rg-16168	rg-442	S6	Similar as gra-xxx type, but bidirectional symmetric	The highest height of both face-to-face sides is 4 nm, the divided surface in one semi-section is two part

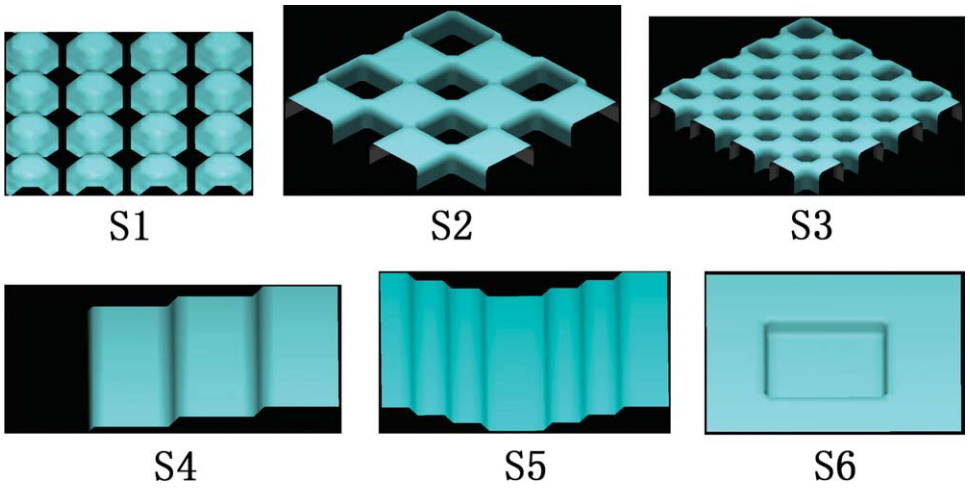

Figure 1 The scheme of six representative inducing surface. [Color figure can be viewed in the online issue, which is available at wileyonlinelibrary.com.]

columns had different sizes and heights to simulate different degrees of surface roughness. The "gra" series were planes with different widths to simulate different degrees of surface roughness. The mask was generated by gradually increasing the column height across the plane, so that it resembled stairs viewed side on. In addition, monodirectional asymmetric planes, such as gra-444 and gra-888, and monodirectional symmetric planes, such as gra-2(444), gra-2(448), and gra-2(888) were considered. The "rg" series were bidirectional symmetric planes originating from monodirectional symmetric planes, as used in the "gra" series. The details about these six types of designed surfaces were listed in Table II, and six representative surfaces (ci-444, co-444, co-884, gra-444, gra-2(444), and rg-442) were showed in Figure 1 as schemes (S1, S2, S3, S4, S5, and S6, respectively).

MesoDyn simulations parameters

The time step of all the MesoDyn calculations was set as 50 ns to stabilize the numerical calculations, the total simulation time was 50 ms for every PS-*b*-PMMA copolymer case. The noise parameter value of 75.002 by default, was used for the numerical speed and stability. The adopted grid dimensions were $32 \times 32 \times 32$ nm^3, and the size of the mesh over which density variations were to be plotted in MesoDyn length unit was 1 nm.

Comparable parameters

The order parameter P was defined as the volume average of the difference between local density squared and the overall density squared, given by the equation

$$P_i = \frac{1}{V}\int_V [\eta_i^2(r) - \eta_i^2]dr$$

where η_i was dimensionless density for species i. The larger the value of the order parameter was, the more obvious the phase separation was. A decrease in P indicated better compatibility or miscibility, and the polymer phases mixed more randomly.

It was necessary to define a comparable parameter, denoted as VROP, which was the abbreviation of the variation rates of order parameters, to discuss the influencing effect of inducing surfaces. Its definition process was: set the plain PS-*b*-PMMA copolymers as a reference, and its order parameter values were named as "*A*"; the order parameter values of PS-*b*-PMMA copolymers induced by surfaces were named as "*B*," then the values of $(B\text{-}A)/A$ were the results of VROP. By comparing the VROP values, we could detect which inducing surface was the effective inducing surfaces on changing the phase morphology of the PS-*b*-PMMA copolymers.

RESULTS AND DISCUSSIONS

Figure 2–5 showed P of six kinds of PS-*b*-PMMA copolymers with eighteen inducing surface effects. Several features could be seen in these figures as follows:

1. In Figure 2 showing the "ci" series surfaces, all the six PS-*b*-PMMA copolymers demonstrated a relationship of $P_{B6A3B6} < P_{B12A6B12} < P_{A3B6} < P_{A6B12} < P_{A3B6A3} < P_{A6B12A6}$, which can be classified into two kinds of main relationship: (a) the first one was $P_{"BAB"} < P_{"AB"} < P_{"ABA"}$. It can be derived when the segment of "A" or "B" located at both sides in copolymers, there were much more opportunity to "meet" with the same kind of segment, then it was easy to form the microscopic areas consisting of the same component, even lead to a microscopic separation. In addition, the weight percentage values of "A" were 20.87%,

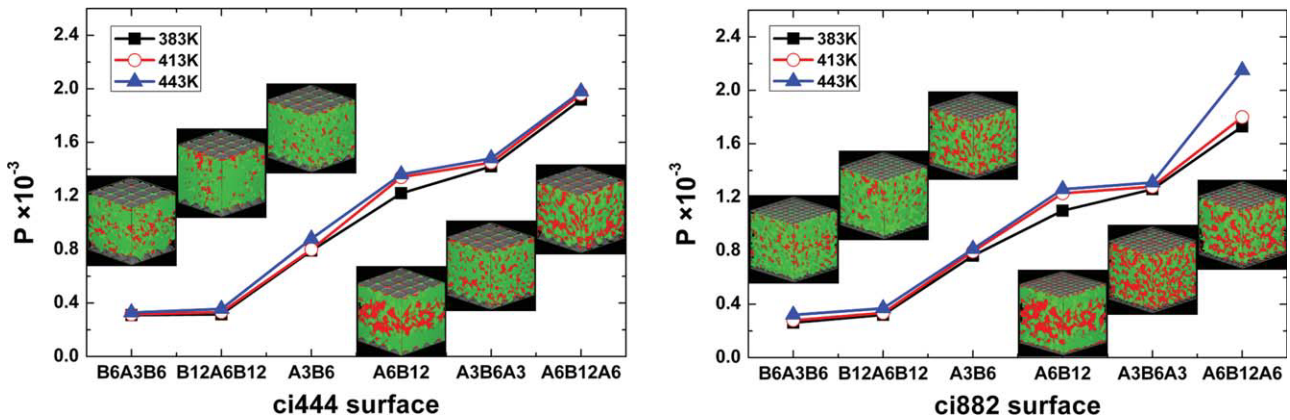

Figure 2 The order parameter values of PS-*b*-PMMA copolymers with ci-444 and ci-882 surface induced at 383, 413, and 443 K. Representative isodensity surface pictures of PS-*b*-PMMA copolymer at 443 K was displayed in the chart, respectively. Red, PS segment; green, PMMA segment. [Color figure can be viewed in the online issue, which is available at wileyonlinelibrary.com.]

33.99%, and 50.96% for "BAB," "AB," and "ABA," respectively. They were all resulted from the difference in the copolymer-type. (b) the second one was $P_{B6A3B6} < P_{B12A6B12}$, $P_{A3B6} < P_{A6B12}$ and $P_{A3B6A3} < P_{A6B12A6}$, which could be reduced as $P_{short\text{-}chained} < P_{long\text{-}chained}$. It also could be attributed to the structure of copolymers, the longer chain formed larger congregation areas than the shorter ones.

For each kind of copolymers, the P values at higher temperature was higher than that at lower temperature, which was a relation of $P_{383\ K} < P_{413\ K} < P_{443\ K}$. It revealed that it was likely to form microscopic separation under higher temperature. Deduced from the high P value at 443 K, compared with it at 383 K and 413 K for every copolymer, high temperature could lead the copolymer present microscopic separation easily, especially for the longer chained copolymer of "ABA" group, induced by ci-888 surface, such as A6B12A6 copolymer.

2. In Figure 3 showing the "co" series surfaces, all the six PS-*b*-PMMA copolymers demonstrated a relationship the same as it induced by "ci" surfaces, except the cases of the six PS-*b*-PMMA copolymers induced by co-4432 and co-8832 surfaces.

   For the copolymers induced by co-4432 surface, it showed a relationship of $P_{B6A3B6} < P_{A3B6A3} < P_{A3B6} < P_{A6B12} < P_{B12A6B12} < P_{A6B12A6}$. It also could be classified into three relationships: (a) $P_{short\text{-}chained} < P_{long\text{-}chained}$ for each group, the reason had been mentioned above. (b) For short-chained copolymers, $P_{B6A3B6} < P_{A3B6A3} < P_{A3B6}$, that was, $P_{"BAB"} < P_{"ABA"} < P_{"AB"}$. The co-4432 surface had discontinuous mask distributions, which meant that the polymer did not have enough room to move and spread; they could only adjust themselves in the "small cubic spaces" formed by neighboring column masks, form a microscopic area consisting of the same segments, even form phase separation. Therefore, the longer chained "BAB" and "ABA" group copolymers presented lower P values. On the contrary, the short chained "AB" group copolymer was more flexible than the longer chained "BAB" and "ABA" to adjust its position, then to form a microscopic area consisting of the same segments, so the P values of "AB" group presented the highest values. (c) However, for long-chained copolymers, $P_{A6B12} < P_{B12A6B12} < P_{A6B12A6}$, that was, $P_{"AB"} < P_{"BAB"} < P_{"ABA"}$, which was different from the short chained copolymer. It mainly attributed to the difference in the chain length. "BAB" and "ABA" of long chained copolymers could have much more opportunity to form ordered microscopic area, compared with the short chained copolymers.

   For the copolymers induced by co-8832 surface, it showed extremely high P value for A6B12A6 copolymer at 383 K, 413 K and 443 K, compared with the other copolymers. The reason was the same as the highest P values of "ABA" induced by "ci" series surface.

3. In Figure 4 showing the "gra" series surfaces, all the six PS-*b*-PMMA copolymers demonstrated a relationship the same as it induced by "ci" surfaces. But there was a little difference between gra-xxx and gra-2(xxx) series surfaces. The differences of P values at different temperatures induced by gra-xxx surfaces were a little larger than it induced by gra-2(xxx) surfaces, except the A6B12A6 copolymer induced by gra-2(888) surface. This was the result from the difference in the inducing surface, that was, gra-xxx surfaces were monodirectional asymmetric and gra-2(xxx) surfaces were monodirectional symmetric.
4. In Figure 5 showing the "rg" series surfaces, all the six PS-*b*-PMMA copolymers demonstrated a relationship similar as it induced by "gra" surfaces. It can be deduced from the origination of the "rg" series surfaces, which was bidirectional symmetric surfaces, compared with "gra" surfaces.

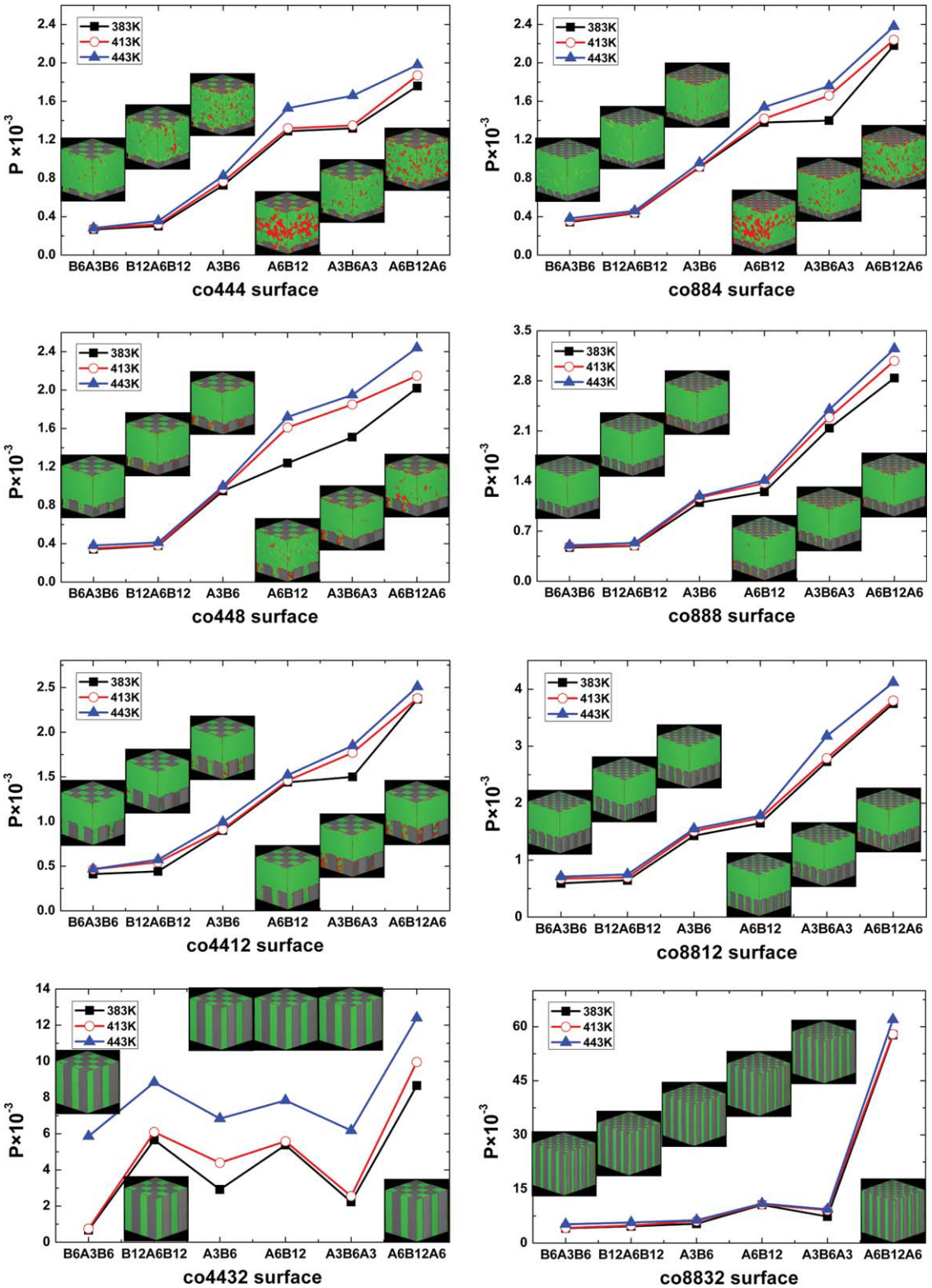

Figure 3 The order parameter values of PS-*b*-PMMA copolymers with co-444, co-448, co-4412, co-4432, co-884, co-888, co-8812, and co-8832 surface induced at 383, 413, and 443 K. Representative isodensity surface pictures of PS-*b*-PMMA copolymer at 443 K was displayed in the chart, respectively. Red, PS segment; green, PMMA segment. [Color figure can be viewed in the online issue, which is available at wileyonlinelibrary.com.]

Figures 6–9 showed VROP values of six kinds of PS-*b*-PMMA copolymers with eighteen inducing surface effects mentioned above, based on the plain copolymers. The VROP values can be applied to illuminate the extent of inducing effect on changing the phase morphology of PS-*b*-PMMA copolymers with

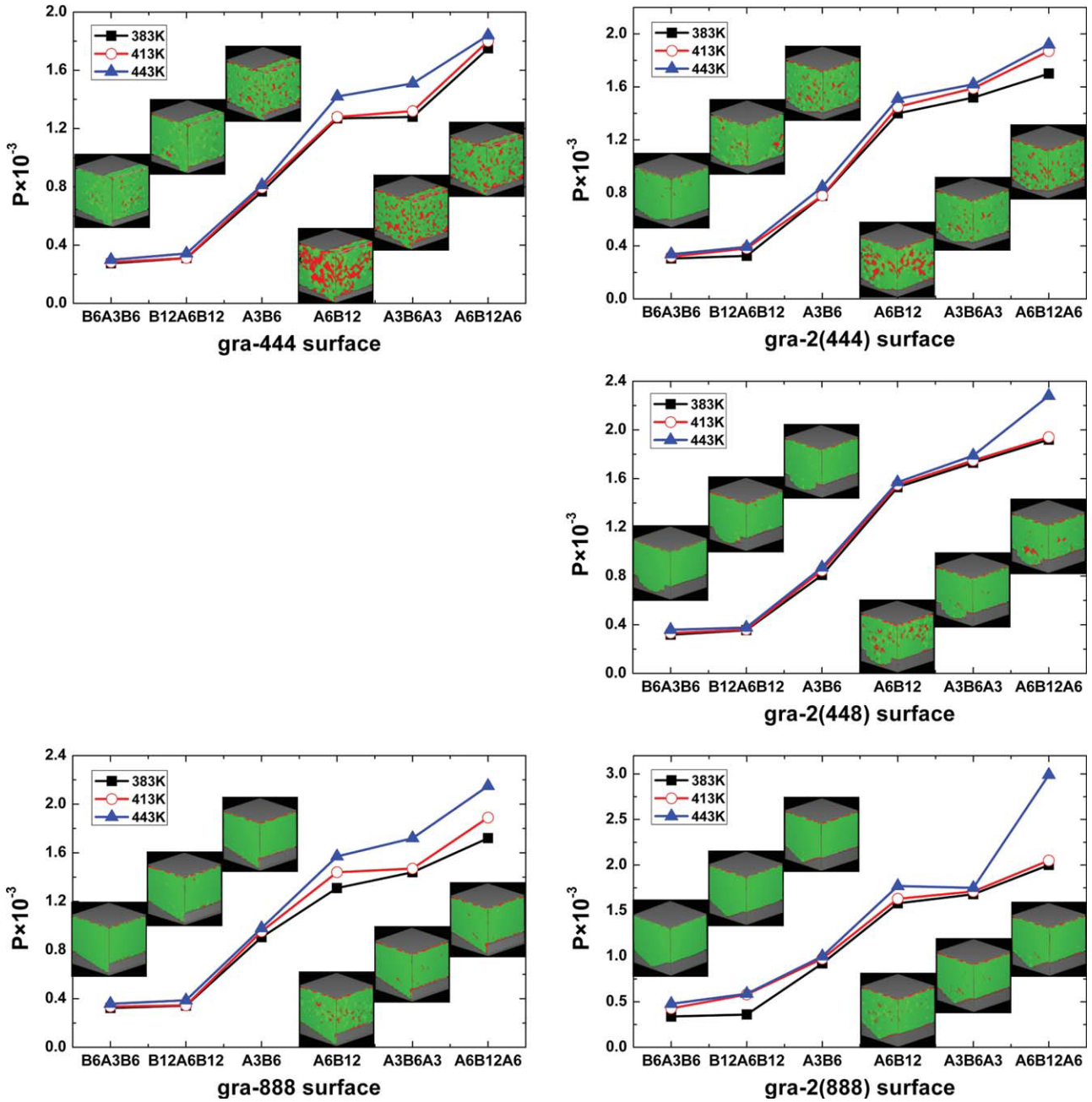

Figure 4 The order parameter values of PS-*b*-PMMA copolymers with gra-444, gra-888, gra-2(444), gra-2(448), and gra-2(888) surface induced at 383, 413, and 443 K. Representative isodensity surface pictures of PS-*b*-PMMA copolymer at 443 K was displayed in the chart, respectively. Red, PS segment; green, PMMA segment. [Color figure can be viewed in the online issue, which is available at wileyonlinelibrary.com.]

18 surfaces induced. A reference line was drawn through the VROP value of 1 in these four figures; when an VROP value lay above the line, the inducing effect was considered a reinforcing immiscible effect; otherwise, the inducing effect was considered a weakening immiscible effect, in addition, the VROP values below zero were considered reinforcing miscible effect. Such reinforcing immiscible and reinforcing miscible effect of six PS-*b*-PMMA copolymers induced by each inducing surface at 383, 413, and 443 K was listed in Table III in details. There were several striking features of these data in Table III, combined with Figures 6–9:

1. The trends seen in these four figures were similar, except it induced by co-4432 and co-8832. It can be deduced from the different structure between these two (co-4432 and co-8832) and the others surfaces. The "ci," "co," "gra," and "rg" surfaces except co-4432 and co-8832 had continuous mask distributions, similar as the situation of its plain copolymers without

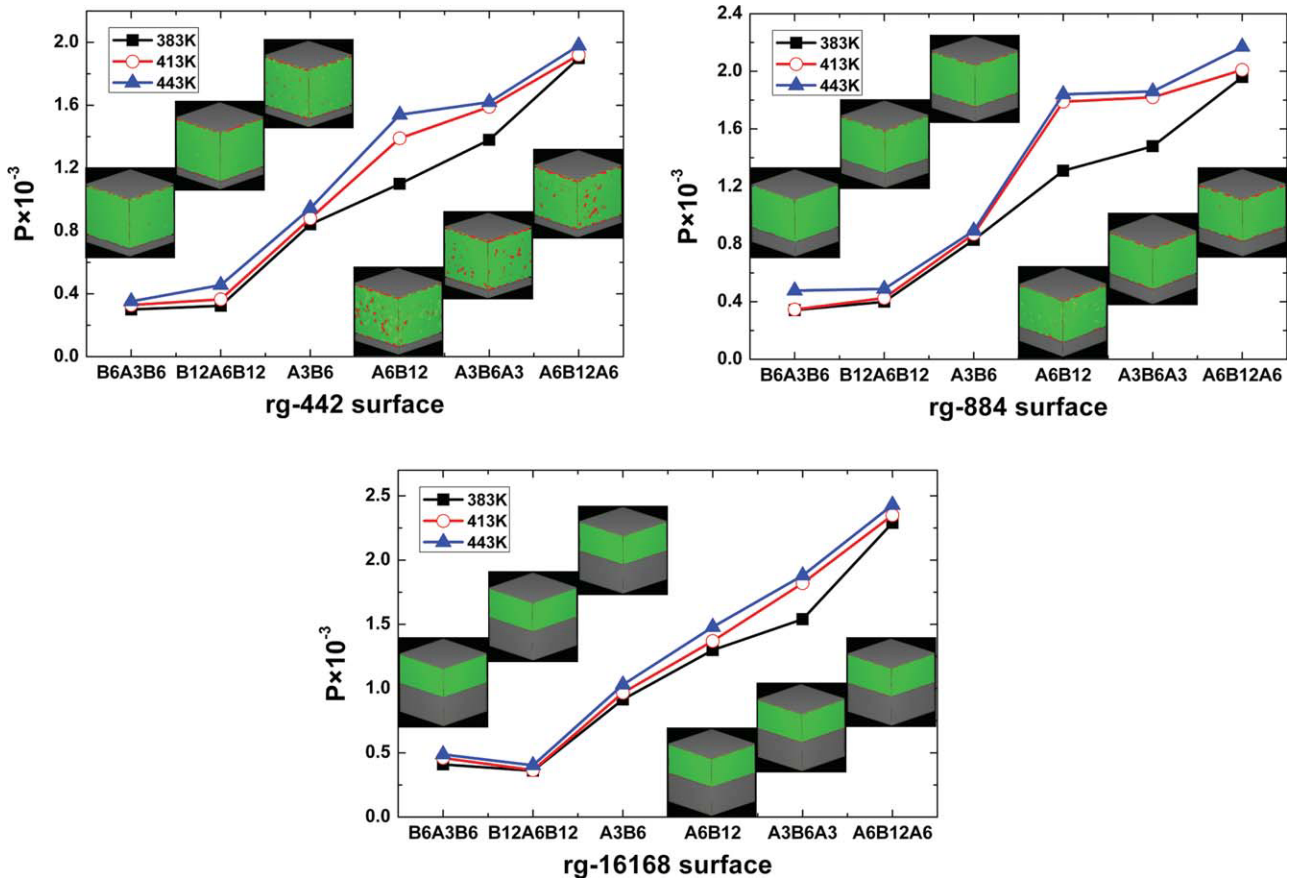

Figure 5 The order parameter values of PS-*b*-PMMA copolymers with rg-442, rg-884, and rg-16168 surface induced at 383, 413, and 443 K. Representative isodensity surface pictures of PS-*b*-PMMA copolymer at 443 K was displayed in the chart, respectively. Red, PS segment; green, PMMA segment. [Color figure can be viewed in the online issue, which is available at wileyonlinelibrary.com.]

surface induced, which allowed the PS-*b*-PMMA copolymers to move and spread more freely until they could adjust themselves to reach stable phase separation. In contrast, the co-4432 and co-8832 had discontinuous mask distributions, which made the copolymer do not have enough room to move and spread; they could only adjust themselves in the "small cubic spaces" formed by neighboring column masks. Therefore, the VROP values of copolymers with co-4432 and co-8832 surfaces induced were all above 1 at 383, 413, and 443 K, furthermore, their values were one order of magnitude higher than the values of other surfaces, which meant

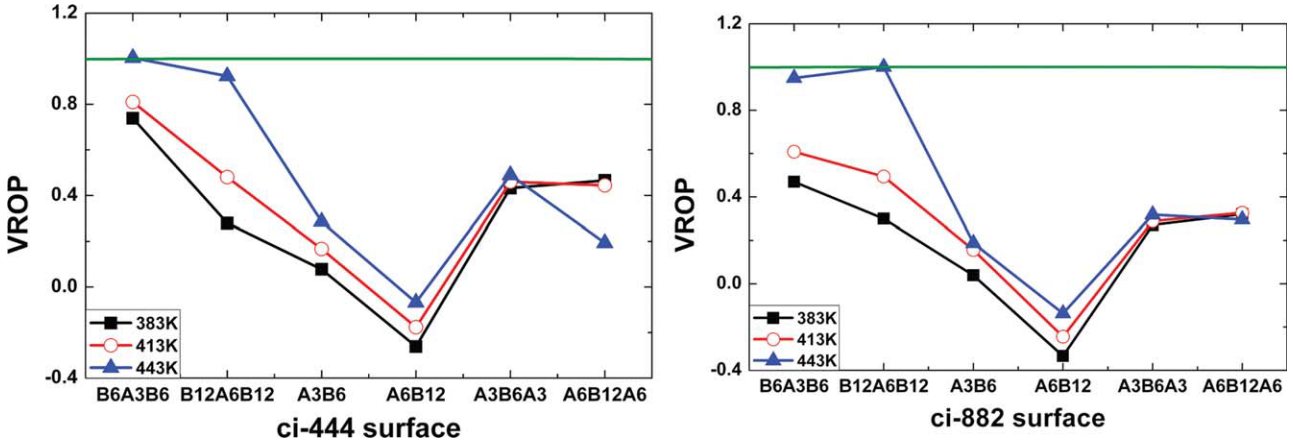

Figure 6 VROP data for PS-*b*-PMMA copolymers induced by ci-444 and ci-882 surface at 383, 413, and 443 K. [Color figure can be viewed in the online issue, which is available at wileyonlinelibrary.com.]

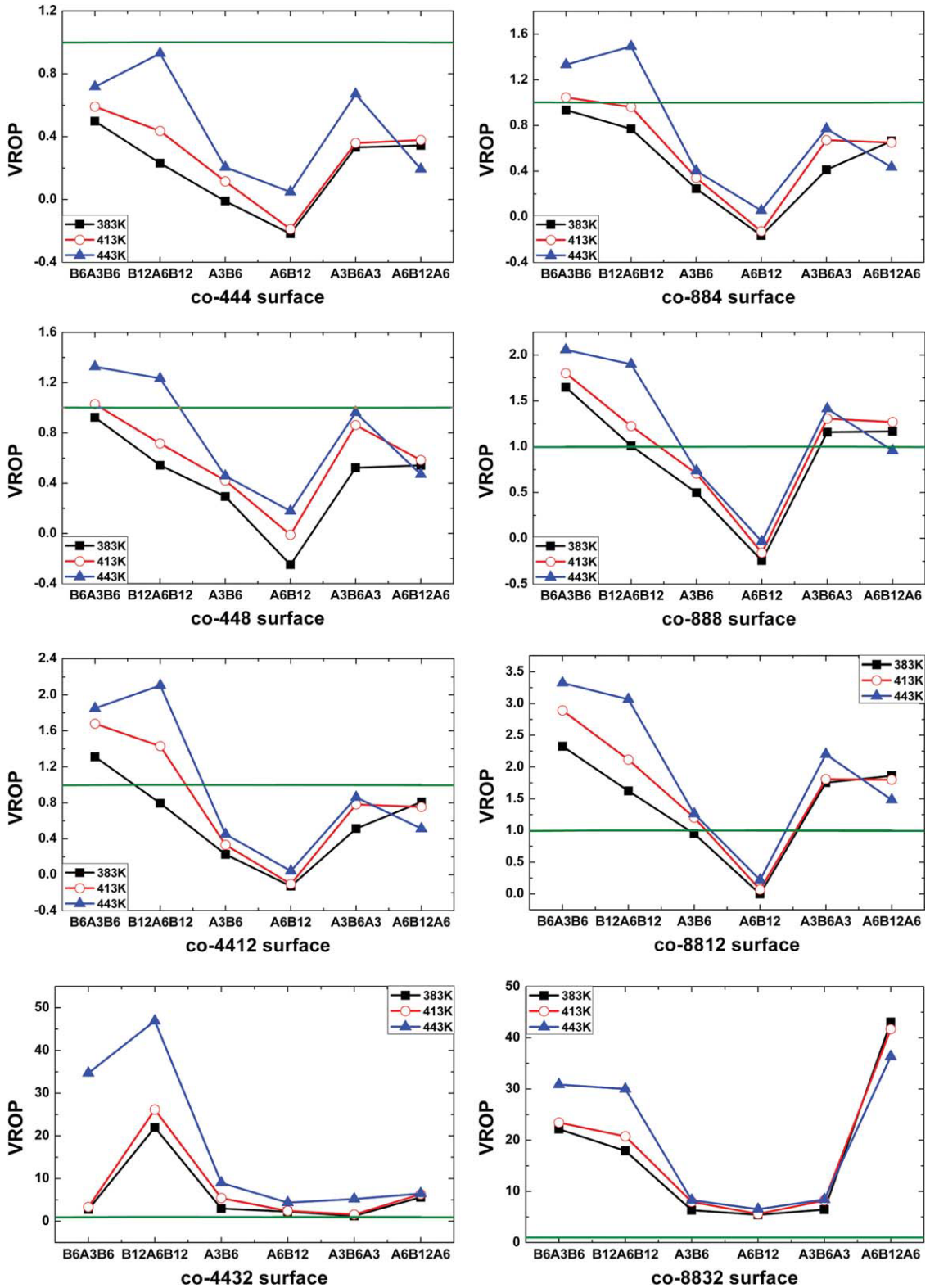

Figure 7 VROP data for PS-*b*-PMMA copolymers induced by co-444, co-448, co-4412, co-4432, co-884, co-888, co-8812, and co-8832 surface at 383, 413, and 443 K. [Color figure can be viewed in the online issue, which is available at wileyonlinelibrary.com.]

such two surfaces played an extreme reinforcing immiscible effect.

2. The number of the case above 1 at 383, 413, and 443 K was 22, 28, and 41, respectively, which was in rising trend; whereas the number of the case below zero at 383, 413, and 443 K was 15, 13, and 4, respectively, which was in decreasing trend. It meant the temperature

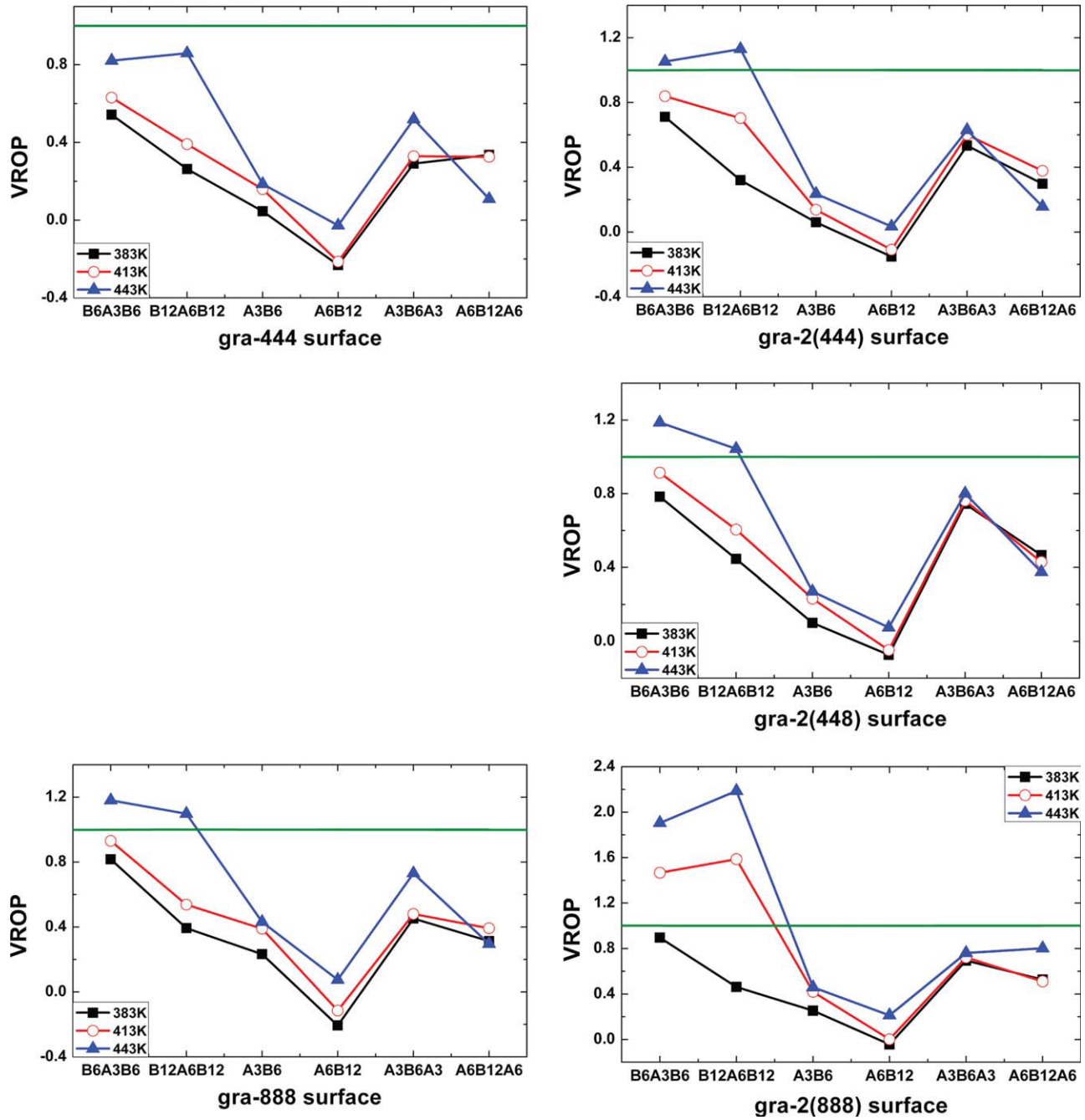

Figure 8 VROP data for PS-*b*-PMMA copolymers induced by gra-444, gra-888, gra-2(444), gra-2(448), and gra-2(888) surface at 383, 413, and 443 K. [Color figure can be viewed in the online issue, which is available at wileyonlinelibrary.com.]

played important role in changing the degrees of phase separation. It can be deduced mainly from the big difference between the diffusion abilities of PS and PMMA segments.[40]

3. The blank of "cases above 1 in. in the table meant the surface played a small role in inducing phase separation, that was, ci-444, ci-882, co-444, co-448, co-884, gra-444, gra-888, gra-2(444), gra-2(448) gra-2(888) rg-442, and rg-884 at 383 K; ci-444, ci-882, co-444, gra-444, gra-888, gra-2(444) gra-2(448) rg-442 and rg-884 at 413 K; ci-882, co-444, gra-444 at 443 K. Among them, the VROP values of ci-882, co-444, and gra-444 surfaces were all below 1 at 383, 413, and 443 K, this meant such three surfaces had little effect on changing the phase morphology of copolymers. It was the result from their relative smooth surface that led them to present little inducing effects.

CONCLUSIONS

Mesoscopic simulations were carried out on PS-*b*-PMMA copolymers with surfaces factored in. The simulation results showed that four series surfaces

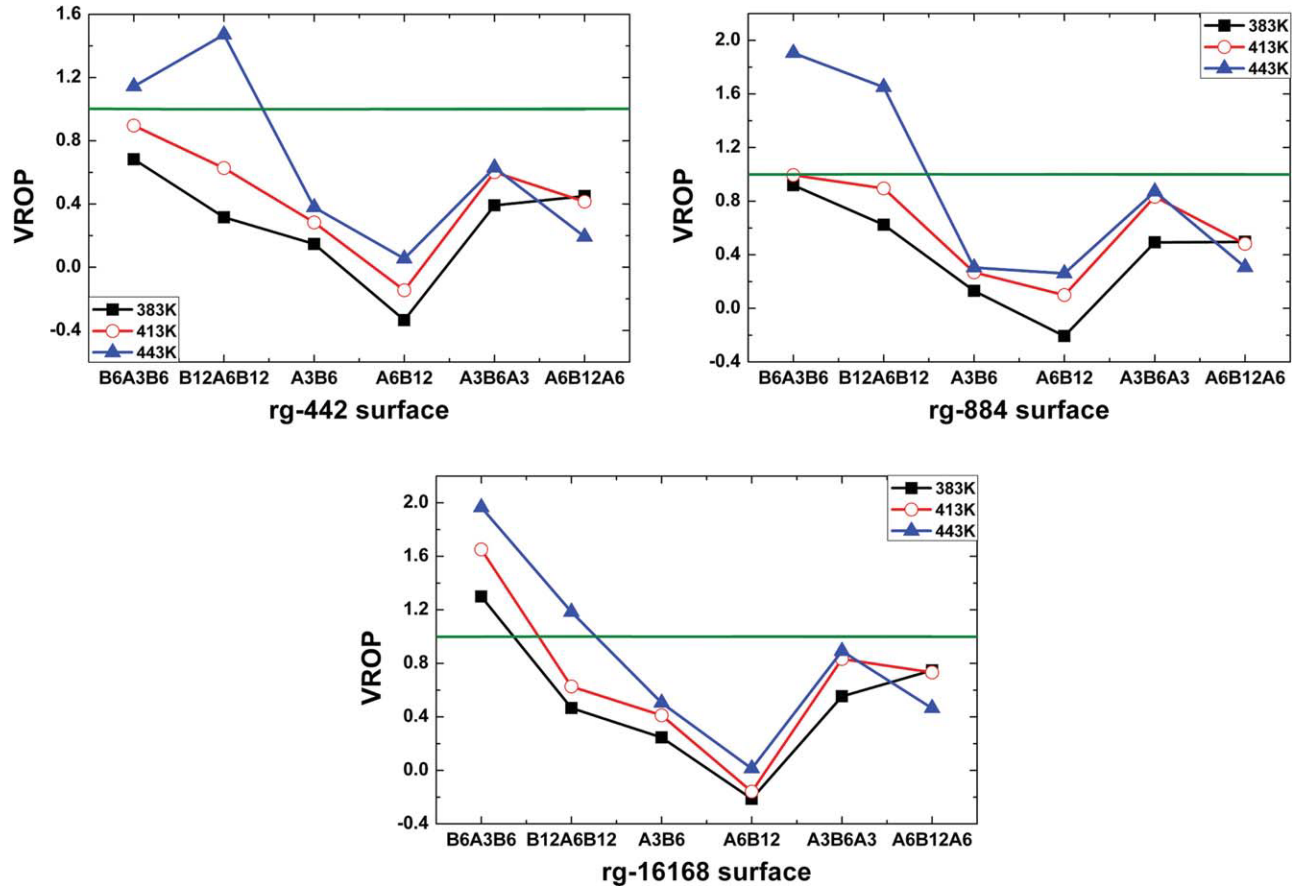

Figure 9 VROP data for PS-*b*-PMMA copolymers induced by rg-442, rg-884, and rg-16168 surface at 383, 413, and 443 K. [Color figure can be viewed in the online issue, which is available at wileyonlinelibrary.com.]

presented different effect on improving the degree of order in the microscopic phases, especially effective on the "ABA" groups copolymers, "AB" groups the second and "BAB" groups the last. In addition, the values of order parameter of the long chains were higher than those of the short ones.

TABLE III
The Classified Information of VROP Values from Figures 6–9 at 383, 413, and 443 K

Surface	Case>1 at 383 K	Case<0 at 383 K	Case>1 at 413 K	Case<0 at 413 K	Case>1 at 443 K	Case<0 at 443 K
ci-444		A6B12		A6B12	B6A3B6	A6B12
ci-882		A6B12		A6B12		A6B12
co-444		A6B12		A6B12		
co-448		A6B12	B6A3B6	A6B12	B12A6B12, B6A3B6	
co-4412	B6A3B6	A6B12	B12A6B12, B6A3B6	A6B12	B12A6B12, B6A3B6	
co-4432	all the cases		all the cases		all the cases	
co-884		A6B12	B6A3B6	A6B12	B12A6B12, B6A3B6	
co-888	B12A6B12, B6A3B6, A6B12A6, A3B6A3	A6B12	B12A6B12, B6A3B6, A6B12A6, A3B6A3	A6B12	B12A6B12, B6A3B6, A3B6A3	A6B12
co-8812	B12A6B12, B6A3B6, A6B12A6, A3B6A3		B12A6B12, B6A3B6, A6B12A6, A3B6A3, A3B6		B12A6B12, B6A3B6, A6B12A6, A3B6A3, A3B6	
co-8832	all the cases		all the cases		all the cases	
gra-444		A6B12		A6B12		A6B12
gra-888		A6B12		A6B12	B12A6B12, B6A3B6	
gra-2(444)		A6B12		A6B12	B12A6B12, B6A3B6	
gra-2(448)		A6B12		A6B12	B12A6B12, B6A3B6	
gra-2(888)		A6B12	B12A6B12, B6A3B6		B12A6B12, B6A3B6	
rg-442		A6B12		A6B12	B12A6B12, B6A3B6	
rg-884		A6B12			B12A6B12, B6A3B6	
rg-16168	B6A3B6	A6B12	B6A3B6	A6B12	B12A6B12, B6A3B6	

The designed "ci," "co," "gra," and "rg" except co-4432 and co-8832 surfaces had continuous mask distributions, which are different from co-4432 and co-8832 surfaces, which had discontinuous mask distributions. Therefore, no matter which temperature was considered, the surfaces had a stronger influence on changing the phase morphology of copolymers, especially the co-4432 and co-8832 surfaces, which performed the most intensive extent of inducing effect on changing the phase morphology of PS-*b*-PMMA copolymers. Higher temperature showed a more obvious effect on changing the phase morphology, but it was not an effective factor on changing the *P* values.

References

1. Stupp, S. I. Curr Opin Colloid Interface Sci 1998, 3, 20.
2. Mao, G.; Ober, C. K. Handbook of Liquid Crystals, Vol3, Wiley-VCH: Weinheim, 1998.
3. Gallot, B. Prog Polym Sci 1996, 21, 1035.
4. Loos, K; Munoz-Guerra, S. Supermolecular Polymers, Dekker: New York, 2000.
5. Kim, K. H.; Huh, J.; Jo, W. H. Macromolecules 2004, 37, 676.
6. Cheng, C. X.; Huang, Y.; Tang, Y. P.; Cheng, E. Q.; Xi, F. Macromolecules 2005, 38, 3044.
7. Kim, J. K.; Hong, M. K.; Ahn, J. H.; Lee, M. Angew Chem Int Ed 2005, 44, 328.
8. Bae, J.; Kim, J. K.; Oh, N. K.; Lee, M. Macromolecules 2005, 38, 4226.
9. Alsunaidi, A.; den Otter, W. K.; Clarke, J. H. R. Philos Trans R Soc Londer Ser A 2004, 362, 1773.
10. Masten, M. W.; Barrett, C. J Chem Phys 1998, 109, 4108.
11. Casey, A.; Harrowell, P. J Chem Phys 1999, 110, 12183.
12. van Duijineveldt, J. S.; Gil-Villegas, A.; Jackson, G.; Allen, M. P. J Chem Phys 2000, 112, 9092.
13. Diplock, R.; Sullivan, D. E.; Jaffer, K. M.; Opps, S. B.,Phys Rev E 2004, 69, 062701.
14. Hamley, I. W. Nanotechnology 2003, 14, R39.
15. Hamley, I. W. The Physics of Block Copolymers; Oxford University Press: Oxford, 1998.
16. Bucknall, D. G.; Anderson, H. L. Science 2003, 3021904.
17. Matsen, M. W.; Schick, M. Phys Rev Lett 1994, 72, 2660.
18. Chen, J. T.; Thomas, E. L.; Ober, C. K.; Mao, G. Science 1996, 273, 343.
19. Jenekhe, S. A.; Chen, X. L. Science 1998, 279, 1903.
20. Jenekhe, S. A.; Chen, X. L. Science 1999, 283, 372.
21. Lee, M.; Cho, B.; Zin, W. Chem Rev (Washington, DC) 2001, 101, 3869.
22. Paul, D. R.; Newman, S. Polymer Blends, Academic Press: New York, 1978.
23. Abd-El-Messieh, S. L. Polym Plast Technol Eng 2003, 42, 153.
24. Schneider, I. A.; Calugaru, E. M. Eur Polym Mater 1976, 12, 879.
25. Bada, R.; Perez Jubindo, M. A.; De, L. A.; Fuente, M. R. Mater Chem Phys 1987, 18, 359.
26. Zhu, P. P. Eur Polym Mater 1997, 33, 411.
27. Lee, J. K.; Han, C. D. Polymer 1999, 40, 6277.
28. Lee, C. F. Polymer 2000, 41, 1337.
29. Li, X.; Han, Y. C.; An, L. J. Polymer 2003, 44, 8155.
30. Walheim, S.; Boltau, M.; Mlynek, J.; Krausch, G.; Steiner, U. Macromolecules 1997, 30, 4995.
31. Schmidt, J. J.; Gardella, J. A., Jr.; Salvati, L., Jr. Macromolecules 1989, 22, 4489.
32. Mu, D.; Li, J. Q.; Zhou, Y. H. J Mol Model 2011, 17, 607.
33. Valls, O. T.; Farrell, J. E. Phys Rev E 1993, 47, R36.
34. Ramirez-Piscina, L.; Hernandéz-Machado, A.; Sancho, J. M. Phys Rev B 1993, 48, 125.
35. Kawakatsu, T.; Kawasaki, K.; Furusaka, M.; Okabayashi, H.; Kanaya, T. J Chem Phys 1993, 99, 8200.
36. Shinozaki, A.; Oono, Y. Phys Rev E 1993, 48, 2622.
37. Fraaije, J. E. M. J Chem Phys 1993, 99, 9202.
38. Fraaije, J G. E. M.; van Vlimmeren, B. A. C.; Maurits, N. M.; Postma, M.; Evers, O. A.; Hoffman, C.; Altevogt, P.; Goldbeck-Wood, G.,J Chem Phys 1997, 106, 4260.
39. Jawalkar, S. S.; Adoor, S. G.; Sairam, M.; Nadagouda, M. N.; Aminabhavi, T. M., J Phys. Chem B 2005, 109, 15611.
40. Mark, J. E., Polymer Data Handbook. Oxford University Press, New York 1999.